

Application of chemical derivatization techniques combined with chemical ionization mass spectrometry to detect stabilized Criegee intermediates and peroxy radicals in the gas phase

Alexander Zaytsev¹, Martin Breitenlechner¹, Anna Novelli², Hendrik Fuchs², Daniel A. Knopf³, Jesse H. Kroll⁴, and Frank N. Keutsch^{1,5,6}

¹John A. Paulson School of Engineering and Applied Sciences, Harvard University, Cambridge, MA 02138, USA

²Institute of Energy and Climate Research – Troposphere (IEK-8), Forschungszentrum Jülich GmbH, 52428 Jülich, Germany

³School of Marine and Atmospheric Sciences, Stony Brook University, Stony Brook, NY 11794, USA

⁴Department of Civil and Environmental Engineering, Massachusetts Institute of Technology, Cambridge, MA 02139, USA

10 ⁵Department of Chemistry and Chemical Biology, Harvard University, Cambridge, MA 02138, USA

⁶Department of Earth and Planetary Sciences, Harvard University, Cambridge, MA 02138, USA

Correspondence to: Alexander Zaytsev (zaytsev@g.harvard.edu) and Frank N. Keutsch (keutsch@seas.harvard.edu)

Abstract. Short-lived highly reactive atmospheric species, such as organic peroxy radicals (RO₂) and stabilized Criegee intermediates (SCIs), play an important role in controlling the oxidative removal and transformation of many natural and anthropogenic trace gases in the atmosphere. Direct speciated measurements of these components are extremely helpful for understanding their atmospheric fate and impact. We describe the development of an online method for measurements of SCIs and RO₂ in laboratory experiments using chemical derivatization and spin trapping techniques combined with H₃O⁺ and NH₄⁺ chemical ionization mass spectrometry (CIMS). Using chemical derivatization agents with low proton affinity, such as electron-poor carbonyls, we scavenge all SCIs produced from a wide range of alkenes without depleting CIMS reagent ions. Comparison between our measurements and results from numeric modelling, using a modified version of the Master Chemical Mechanism, shows that the method can be used for quantification of SCIs in laboratory experiments with detection limit of 1.4×10^7 molecule cm⁻³ for 30 s integration time with the instrumentation used in this study. We show that spin traps are highly reactive towards atmospheric radicals and form stable adducts with them by studying the gas-phase kinetics of their reaction with hydroxyl radical (OH). We also demonstrate that spin trap adducts with SCIs and RO₂ can be simultaneously probed and quantified under laboratory conditions with detection limit of 1.6×10^8 molecule cm⁻³ for 30 s integration time for RO₂ species with the instrumentation used in this study. Spin trapping prevents radical secondary reactions and cycling, which ensures that measurements are not biased by chemical interferences, and can be implemented for detecting RO₂ species in the ambient atmosphere.

1 Introduction

30 Earth's atmosphere is an oxidizing environment. The initial oxidation step of volatile organic compounds (VOCs) involves reaction of a parent hydrocarbon with an oxidant. The hydroxyl radical (OH) is the most important oxidant in the atmosphere,

although oxidation can be also initiated by O₃, NO₃ and Cl- or Br-atoms. Generally, reaction of VOCs with OH, NO₃ and Cl-atoms occurs via H-abstraction or via addition to unsaturated carbon double bonds leading to the formation of alkyl radicals. This reaction is quickly followed by O₂ addition resulting in the production of organic peroxy radicals (RO₂). In an NO-rich environment, RO₂ radicals predominantly react with NO, while at lower NO concentrations reactions with the hydroperoxy radical (HO₂), potentially other RO₂, and unimolecular reactions become more important. The common tendency is the formation of closed-shell, more oxidized VOCs (OVOCs). OVOCs may have lower volatilities than the parent hydrocarbons and may partition to the particle phase, thereby contributing to secondary organic aerosol (SOA) formation. OH, HO₂ and RO₂ radicals can form a catalytic reaction cycle, which can lead to production of tropospheric ozone as a consequence of the shift in the NO/NO₂ ratio to favor formation of NO₂. This cycle is terminated by the formation of organic hydroperoxides and nitrates, which can be viewed as reservoirs of the corresponding radicals. Overall, atmospheric radicals, especially their cycling, play an important role in the formation of SOA and tropospheric ozone, as well as in controlling atmospheric oxidation capacity.

Organic peroxy radicals can also be formed via ozonolysis of unsaturated organic compounds. Ozonolysis of alkenes results in the formation of primary ozonides that promptly decompose to a stable carbonyl and a vibrationally excited carbonyl oxide, also known as a Criegee intermediate (CI), some of which are thermally stabilized (SCI). SCI primarily decompose or react with water vapor (Vereecken et al., 2017) but are also believed to play a role in oxidation of SO₂ to form H₂SO₄ in the tropical regions (Khan et al., 2018). *syn*-SCI can undergo a unimolecular reaction and form a vinyl hydroperoxide, which rapidly decomposes to an OH radical and a vinyl radical. This radical is in resonance with an acetyl-type radical, which can combine with molecular oxygen to form an RO₂ species (Johnson and Marston, 2008).

Measurements of atmospheric radicals and reactive intermediates, such as RO₂ and SCIs, are challenging because of their high reactivity towards trace gases and surfaces and rapid cycling, which may lead to potential interferences. Highly sensitive detection systems are required to determine the minute concentrations of these species. Concentrations of the smallest organic peroxy radicals, CH₃O₂, are typically on the order of 10⁸ molecule cm⁻³ while concentrations of other RO₂ species can be much lower (Fuchs et al., 2008). As for SCIs, their concentrations are expected to be less than 10⁵ molecule cm⁻³ (Novelli et al., 2017). With respect to RO₂ species, there are several field-deployable measurement techniques available for non-speciated measurements of the sum of RO₂. Matrix Isolation Electron Spin Resonance Spectroscopy (MIESR) is an established, but rarely used, method for field measurements (Mihelcic et al., 1985). MIESR is an offline technique with a low time resolution (~30 min), however, its main advantage is that it does not require instrument calibration. Besides MIESR, chemical amplification and conversion systems represent another class of instruments for field studies (Edwards et al., 2003; Hornbrook et al., 2011; Cantrell et al., 1984; Wood and Charest, 2014). In these systems peroxy radicals are not measured directly but are rather converted to other radicals or closed-shell molecules (e.g., NO₂ or H₂SO₄). A detection limit of 10⁷ molecule cm⁻³ can be achieved at a temporal resolution of 15 s, however, discrimination of different RO₂ species is not possible (Edwards et al., 2003). In addition, secondary chemistry, i.e., additional sources of radical production and destruction, has to be considered, and care needs to be taken to ensure that measurements are not biased by any chemical interferences (Reiner et al., 1997).

Finally, laser-induced fluorescence (LIF) was also applied for ambient measurements of RO₂ radicals (Fuchs et al., 2008). This technique is characterized by an excellent detection limit of $(2 - 7) \times 10^7$ molecule cm⁻³ for an integration time of 30 s. Similarly to chemical amplifier systems, LIF does not allow for differentiation of various RO₂ species, however, although it is indirect and converts RO₂ to OH it does not have an amplification chain. Recently, novel mass spectrometric techniques using different ionization schemes to directly detect individual RO₂ species were developed (Hansel et al., 2018; Berndt et al., 2018; Berndt et al., 2019; Nozière and Vereecken, 2019).

As for SCIs, indirect measurement techniques have been widely used. In these techniques SCIs are chemically converted to other species (e.g., H₂SO₄ or hydroxymethyl hydroperoxide, HMHP) (Berndt et al., 2014; Sipilä et al., 2014; Neeb et al., 1997). In 2008, the simplest SCI, CH₂OO, was directly detected for the first time (Taatjes et al., 2008). Later, synchrotron photoionization mass spectrometry was combined with the CI generation technique using diiodoalkane photolysis (Welz et al., 2012), which spurred several studies to examine kinetics of bimolecular and unimolecular SCI reactions (Taatjes et al., 2012; Lewis et al., 2015; Chhantyal-Pun et al., 2016). Recently two new techniques for direct measurements of SCIs using Fourier transform microwave spectroscopy and chemical ionization mass spectrometry (CIMS) were introduced (Womack et al., 2015; Berndt et al., 2017).

Despite the abundance of different analytical methods used for detection of atmospheric radicals and reactive intermediates, there is still a need for an online, direct, field-deployable technique for measuring these short-lived highly reactive compounds in a speciated way. Free radicals have been conventionally detected by chemical derivatization (CD) techniques including spin trapping in condensed-phase biological and chemical systems (Hawkins and Davies, 2014; Nosaka and Nosaka, 2017). Non-radical spin traps (e.g., nitron spin traps) are known to react with free radicals to form stable radical adducts that can be detected with electron paramagnetic resonance spectroscopy (Roberts et al., 2016). In addition, radical spin traps (e.g., nitroxide radicals) are also highly reactive towards radical species such as C-centered radicals and form closed-shell adducts with them (Bagryanskaya and Marque, 2014). However, there are only few studies in which these techniques were applied for probing atmospheric radicals and intermediates. Watanabe et al. (1982) presented an offline method to quantify hydroxyl radicals using the spin trap α -4-pyridyl-*N*-*tert*-butylnitron α -1-oxide (4-POBN) where condensed-phase stable adducts were detected by electron spin resonance. Recently, Giorio et al. (2017) used the spin trap 5,5-Dimethyl-1-pyrroline *N*-oxide (DMPO) to characterize SCIs by detecting gas-phase spin trap adducts with online mass spectrometry.

Here we explore three types of CD agents, including two spin trapping agents, and show how they can be used for detection and quantification of various atmospheric radicals and reactive intermediates (Fig. 1). First, we implement the CD agent hexafluoroacetone (HFA) to characterize a wide range of gas-phase SCIs. HFA is selectively reactive towards SCIs (i.e., it is unreactive towards OH, HO₂ and RO₂), forms stable secondary ozonides with them, and has high vapor pressure and low proton affinity (Fig. 1). Next, we use the radical spin trap (2,2,6,6-Tetramethylpiperidin-1-yl)oxyl (TEMPO) to demonstrate that spin traps are highly reactive towards radicals in the gas phase, by studying kinetics of TEMPO+OH reaction, and therefore can effectively scavenge atmospheric radicals. Finally, we utilize the non-radical spin trap DMPO to simultaneously detect atmospheric gas-phase radicals and intermediates, including SCIs and RO₂ species (Fig. 1). Spin trap adducts and secondary

100 ozonides with CD agents are observed and quantified using H_3O^+ and NH_4^+ CIMS, which allows for speciated online measurements of stabilized Criegee intermediates and speciated RO_2 radicals formed via ozonolysis of a wide range of parent hydrocarbons. The analytical methods presented here can be used for quantification of speciated SCIs and RO_2 formed in laboratory experiments as well as for field measurements.

2 Methods

105 2.1 Ozonolysis experiments with chemical derivatization agent HFA

The ozonolysis experiments of multiple hydrocarbons including tetramethylethylene (TME), isoprene, pentene, hexene, α -pinene and limonene were conducted in a flow tube reactor at ambient pressure and temperature (~ 290 K) and dry conditions (relative humidity $< 2\%$). The experimental setup consisted of a flow reactor system with a residence time of ~ 10 s. The parent hydrocarbon was mixed with ozone and the chemical derivatization agent HFA ($\text{C}_3\text{F}_6\text{O}$) in the flow reactor leading to the
110 formation of SCIs and their scavenging as SCI-HFA adducts. SCIs are known to be highly reactive towards ketones, especially electron poor ones such as HFA (Horie et al., 1999; Taatjes et al., 2012). HFA has been previously used to effectively scavenge SCIs and prevent their secondary chemistry to directly probe SCI formation (Drozd et al., 2011; Drozd and Donahue, 2011). The other advantage of employing this chemical derivatization agent is its relatively low proton affinity (PA 670.4 kJ/mol; Hunter and Lias, 1998). Since the PA of HFA is lower than that of water, HFA cannot be protonated in H_3O^+ CIMS. Hence,
115 one can introduce significant amount of HFA to the system to make sure that all SCIs are scavenged very rapidly without any concern that H_3O^+ reagent ions would be depleted. The parent hydrocarbon was vaporized from a flask filled with pure substance by passing a constant flow of zero air regulated via a $0.1\text{-}10\text{ cm}^3\text{ min}^{-1}$ mass flow controller (Bronkhorst). HFA flow was regulated by another mass flow controller (Bronkhorst). Ozone was produced by passing zero air through an ozone generator using a low-pressure mercury ultraviolet lamp. Ozone concentration was measured using an ozone monitor (2B
120 Technologies) (Table S2).

A proton-transfer-reaction mass spectrometer (PTR-8000, IONICON Analytik) was used to observe formed SCI-HFA adducts as well as parent hydrocarbons and their oxidation products. This instrument was operated using H_3O^+ reagent ions (H_3O^+ CIMS) and was directly calibrated to 10 VOCs with different functional groups (Isaacman-VanWertz et al., 2017; Isaacman-VanWertz et al., 2018).

125 2.2 Experiments with spin traps

2.2.1 Kinetics experiments with spin trap TEMPO

Highly reactive spin traps are needed for effective derivatization of radicals and reactive intermediates in the gas phase. A set of experiments, in which the reaction rate coefficient between the spin trap TEMPO ($\text{C}_9\text{H}_{18}\text{NO}$) and OH was measured, was conducted in a flow tube experimental setup at Forschungszentrum Jülich. TEMPO is commonly used to detect carbon-

130 centered radicals in chemical and biological systems (Bagryanskaya and Marque, 2014) and is known to be highly reactive towards OH in the aqueous phase (Samuni et al., 2002). TEMPO was introduced in the flow tube setup using a liquid calibration unit (LCU, IONICON Analytik). The LCU quantitatively evaporates aqueous standards into the gas stream. TEMPO standard was prepared gravimetrically with aqueous volume mixing ratio of 485 parts per million (ppm). A known amount (up to 10 $\mu\text{L min}^{-1}$) of this solution was then evaporated into a humidified gas stream of synthetic air (31 SLPM), resulting in the gas-
135 phase TEMPO concentration of up to 4.5×10^{11} molecule cm^{-3} . One part of the setup outflow was drawn to a laser photolysis – laser-induced fluorescence (LP-LIF) instrument (Lou et al., 2010), with which OH reactivity of TEMPO was measured. Laser flash photolysis of ozone was used to produce OH in the experimental setup, while LIF was applied to monitor the time dependent OH decay. Another part of the outflow was drawn to a CIMS instrument PTR3 (IONICON Analytik) to monitor concentrations of TEMPO and its oxidation products. This instrument was operated in two ionization modes: using
140 $\text{H}_3\text{O}^+(\text{H}_2\text{O})_n$, $n = 0-1$ (as H_3O^+ CIMS; Breitenlechner et al., 2017) and $\text{NH}_4^+(\text{H}_2\text{O})_n$, $n = 0-2$ (as NH_4^+ CIMS; Zaytsev et al., 2019) reagent ions. The PTR3 is designed to minimize inlet losses of sampled compounds. It was directly calibrated to 10 VOCs with different functional groups using LCU. Collision-dissociation methods were used to constrain sensitivities of NH_4^+ CIMS to compounds that cannot be calibrated directly (Zaytsev et al., 2019). Sensitivities were calculated in normalized duty-cycle-corrected counts per second per part per billion by volume (ndcps ppb^{-1} ; the duty-cycle correction was done to the
145 reference $m/z = 100$; ion signals were normalized to the primary ion signal of 10^6 dcps).

2.2.2 Ozonolysis experiments with spin trap DMPO

An additional set of ozonolysis experiments of several hydrocarbons including TME and α -pinene were conducted in a double flow reactor setup (Fig. 2). The goal of these experiments was to examine how spin traps can be used for simultaneous detection of stabilized Criegee intermediates and peroxy radicals. Experimental setup consisted of two identical $\sim 2.1\text{L}$ flow reactors.
150 The parent hydrocarbon was mixed with ozone in the first flow tube reactor with a residence time of $\sim 28\text{s}$. Similar to the previous ozonolysis experiments described in Sect. 2.1, the parent hydrocarbon was vaporized from a flask filled with pure substance by passing zero air regulated by a mass flow controller, and ozone was generated using a low-pressure mercury ultraviolet lamp. We used an LCU to introduce the spin trap DMPO ($\text{C}_6\text{H}_{11}\text{NO}$) in the second flow reactor with a residence time of $\sim 23\text{s}$. A known amount (up to $10 \mu\text{L min}^{-1}$) of the DMPO solution was evaporated into a humidified gas stream of
155 synthetic air (5.4-7 SLPM), resulting in the gas-phase DMPO concentration of up to 1.1×10^{13} molecule cm^{-3} . The second flow reactor served for derivatization of SCIs and RO_2 species by DMPO while the parent hydrocarbon was still reacting with ozone. Hence, we conducted integrated production measurements of SCIs and RO_2 species formed in both flow reactors. DMPO represents a class of non-radical spin traps and is widely used to detect oxygen-centered radicals, such as OH, HO_2 and RO_2 , in chemical and biological systems (Roberts et al., 2016; Van Der Zee et al., 1996). Recently, DMPO was also employed
160 to detect SCIs in the gas phase (Giorio et al., 2017). The PTR3 was used to detect SCI-DMPO and RO_2 -DMPO adducts, while ozone levels were observed using an ozone monitor (2B Technologies) (Table S3).

2.3 Kinetic model and quantum-chemical calculations

The Framework for 0-D Atmospheric Modelling v3.1 (FOAM; Wolfe et al., 2016) containing reactions from the Master Chemical Mechanism (MCM v3.3.1) (Jenkin et al., 1997; Saunders et al., 2003) was used to simulate photooxidation of studied alkenes in the flow reactor system and to compare the modeled concentrations of the products with the measurements. Model calculations were constrained using physical parameters of the experimental setup (pressure and temperature) as well as to observed concentrations of the parent hydrocarbon, ozone and the chemical derivatization agent.

In order to estimate proton affinities of SCI·HFA adducts, we performed geometry optimization and proton affinity calculations with the Gaussian 09 package (Frisch et al., 2009) using the B3LYP functional (Stephens et al., 1994) and TZVP basis sets.

3 Results and discussion

3.1 Detection of speciated stabilized Criegee intermediates using chemical derivatization techniques

The primary goal of the first set of experiments was detection of speciated stabilized Criegee intermediates as adducts with the chemical derivatization agent HFA to prevent secondary reactions within the experimental setup. Starting with $(\text{CH}_3)_2\text{COO}$, an SCI produced via ozonolysis of TME, we tested the formation of SCI·HFA adducts under different experimental conditions (Fig. 3). $(\text{CH}_3)_2\text{COO}\cdot\text{HFA}$ ($\text{C}_6\text{H}_6\text{O}_3\text{F}_6\cdot\text{H}^+$, m/z 241.03) can be easily identified in the mass-spectrum due to its unique mass defect associated with six F-atoms (Fig. S2). SCI·HFA adducts were observed when TME, ozone, and HFA were present in the experimental setup. Ozonolysis of TME also results in the formation of acetone ($\text{C}_3\text{H}_6\text{O}\cdot\text{H}^+$, m/z 59.05), which was detected in the presence of TME and ozone and was not affected by HFA addition (Fig. 3).

We measured the $(\text{CH}_3)_2\text{COO}\cdot\text{HFA}$ adduct signal as a function of different reactant conditions: initial TME concentration were in the range of $(1.48 - 1.85) \times 10^{11}$ molecule cm^{-3} , ozone, $(6.77 - 108.2) \times 10^{12}$ molecule cm^{-3} , HFA $(1.17 - 6.13) \times 10^{15}$ molecule cm^{-3} . The measurements are compared to the predictions of the kinetic model in Fig. 4. Concentrations of $(\text{CH}_3)_2\text{COO}$ species were calculated using the MCM with updated kinetics data from the literature (Newland et al., 2015; Chhantyal-Pun et al., 2016; Long et al., 2018). For more details see the Supplement.

In the presence of HFA, SCI can react with HFA and form stable adducts:



The reaction rate coefficient k_1 was not measured experimentally, and we used the k -value for $\text{CH}_2\text{OO} + \text{HFA}$ reaction: $k_1 = 3 \times 10^{-11}$ cm^3 molecule $^{-1}$ s $^{-1}$ (Taatjes et al., 2012). It has been suggested that the reaction between HFA and acetone oxide may be slower compared to the CH_2OO one (Murray et al., 1965; Taatjes et al., 2012) while $k_{(\text{CH}_3)_2\text{COO}+\text{HFA}} = 2 \times 10^{-13}$ molecule cm^{-3} s $^{-1}$ was used in the previous studies (Drozd et al., 2011). However, the concentration of HFA was two orders of magnitude higher than concentrations of other chemical compounds, so even at lower k -values reaction with HFA remains the major chemical loss pathway for $(\text{CH}_3)_2\text{COO}$ (Fig. S3).

Observed concentrations of $(\text{CH}_3)_2\text{COO}\cdot\text{HFA}$ agree to within a factor of 3 with concentrations predicted by the kinetic model (Fig. 4). This discrepancy can be explained by a combination of the following factors. First, a fraction of $(\text{CH}_3)_2\text{COO}\cdot\text{HFA}$ adducts might be irreversibly deposited on the surfaces inside the experimental setup and the PTR 8000 instrument (Pagonis et al., 2017). In addition, the sensitivity of observed SCI·HFA adducts depends on the reaction rate constant of the adduct with H_3O^+ ion and the degree of fragmentation of protonated product ions $\text{SCI}\cdot\text{HFA}\cdot\text{H}^+$ (Yuan et al., 2017). Since the reaction rate constant of SCI·HFA with H_3O^+ ions is unknown, we assumed that all SCI·HFA adducts were ionized via proton transfer from hydronium ions and therefore used the sensitivity we obtained from acetone calibration to quantify detected SCI·HFA species. In addition, we did not take into account possible fragmentation of $\text{SCI}\cdot\text{HFA}\cdot\text{H}^+$ ions which may impede their detection, although a first bond cleavage would likely only break the ozonide ring structure without loss of mass. Finally, uncertainty of the kinetic model output is determined by the uncertainty in the SCI yield, and unimolecular and bimolecular reaction rate coefficients. The detection limit for $(\text{CH}_3)_2\text{COO}\cdot\text{HFA}$ adducts was 1.4×10^7 molecule cm^{-3} and was calculated for 30 s integration time as 3 standard deviations of measured background divided by derived sensitivity.

Besides TME, we also observed formation of SCI·HFA for a series of precursors including isoprene, pentene, and hexene. (Figs. S4-S6). Proton affinities (PAs) of different CI·HFA adducts were calculated using DFT methods (Table 1). A variety of these adducts can be detected using H_3O^+ CIMS since their PAs are significantly higher than that of water which is in agreement with experimental data (Figs. S4-S6). $\text{CH}_2\text{OO}\cdot\text{HFA}$ cannot be detected because of its low PA (Table 1). We also did not observe SCI·HFA adducts for larger C_{10} SCIs produced via ozonolysis of α -pinene and limonene. This can be explained by the lower reactivity of larger SCIs with HFA, potential instability of these secondary ozonides in the gas phase, or their gas-wall partitioning in tubing and inside the PTR-8000 instrument.

3.2 Reactivity of spin traps with OH

Spin traps have been shown to be highly reactive towards free radicals and efficiently form adducts with them in the aqueous phase. However, their reactivity with atmospheric radicals and stability of formed adducts in the gas phase remain largely unknown. In order to address these questions, we conducted a set of experiments to estimate the reaction rate between the spin trap TEMPO and the hydroxyl radical by measuring its OH reactivity.

OH reactivity of a specific reactant can be calculated as a product of the reactant concentration and its reaction rate with OH (Fuchs et al., 2017):

$$k_{\text{OH}} = k_{\text{OH}+\text{TEMPO}} \cdot [\text{TEMPO}] \quad (1)$$

k_{OH} was measured as a function of TEMPO concentration by varying the amount of TEMPO introduced in the experimental setup using the LCU (Fig. 5). The slope of the fitted line in Fig. 5 determines the reaction rate coefficient $k_{\text{OH}+\text{TEMPO}} = (9.3 \pm 0.9) \times 10^{-11}$ $\text{cm}^3 \text{ molecule}^{-1} \text{ s}^{-1}$. This rate constant is close to the collisional limit of typical radical-molecule reactions in the atmosphere and is one order of magnitude greater than the rate constant for the same reaction in the aqueous phase ($k_{\text{aqueous}} = 7.5 \times 10^{-12}$ $\text{cm}^3 \text{ molecule}^{-1} \text{ s}^{-1}$; Samuni et al., 2002). This demonstrates that TEMPO is highly reactive towards OH in the gas

phase, emphasizing the applicability of spin trapping for atmospheric measurements. Furthermore, TEMPO + OH reaction
225 leads to the formation of stable TEMPO·OH adducts that can be detected by H₃O⁺ CIMS (C₉H₁₈NO·H⁺, *m/z* 174.149) and
therefore could be used for quantification of hydroxyl radicals in the atmosphere (Fig. S7). Further tests are needed to compare
the measurement capability of this method (e.g., sensitivity, wall losses, and potential interferences) with that of a well-
established technique, such as LIF.

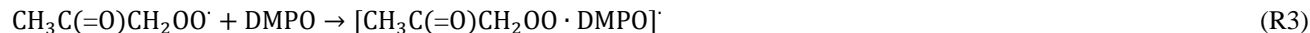
3.3 Simultaneous detection of SCIs and RO₂ species from ozonolysis of alkenes using spin trapping techniques

230 Next, we implemented spin trapping for detection of speciated SCIs and RO₂ species formed via ozonolysis of alkenes, starting
with TME. Decomposition of the TME primary ozonide leads to formation of acetone oxide (CH₃)₂COO. This SCI can further
undergo a unimolecular reaction followed by O₂ addition to form a peroxy radical CH₃C(=O)CH₂OO· and OH (Fig. 1). In
order to detect SCIs and RO₂ species produced via ozonolysis of TME, we used a measurement method based on stabilization
of these species using the spin trap DMPO followed by detection by NH₄⁺ and H₃O⁺ CIMS. DMPO was shown to form stable
235 secondary ozonides with SCIs in the gas phase (Giorio et al., 2017):



DMPO is shown to be highly reactive towards SCIs ($k_{\text{CI}+\text{DMPO}} \geq 6 \times 10^{-11} \text{ cm}^3 \text{ molecule}^{-1} \text{ s}^{-1}$; see the Supplement for more
details).

In addition, DMPO is known to be highly reactive towards oxygen-centered radicals, such as RO₂, and form stable radical
240 adducts with them (Fig. 1):



We observed the formation of SCI·DMPO and RO₂·DMPO adducts both in NH₄⁺ CIMS (e.g., C₉H₁₇NO₃·NH₄⁺, *m/z* 205.155
and C₉H₁₆NO₄·NH₄⁺, *m/z* 220.142) and H₃O⁺ CIMS (e.g., C₉H₁₇NO₃·H⁺, *m/z* 188.128 and C₉H₁₆NO₄·H⁺, *m/z* 203.116) under
different experimental conditions (Figs. 6 and S8). SCI·DMPO and RO₂·DMPO were only detected when TME, ozone, and
245 DMPO were present in the experimental setup. Acetone, also formed via ozonolysis of TME, was observed in the presence of
TME and ozone and was not affected by addition of DMPO (Figs. 6 and S8). OH radicals, formed via decomposition of SCI,
can in turn react with TME and lead to formation of another RO₂ species OH-C₆H₁₂OO·. This radical was detected as the
C₆H₁₃O₃·DMPO adduct (C₁₂H₂₄NO₄, *m/z* 264.205; Fig. 6). One of the benefits of NH₄⁺ CIMS is the possibility of quantifying
compounds for which authentic standards are not available, using a voltage scanning procedure based on collision-induced
250 dissociation (Zaytsev et al., 2019). Based on this method, DMPO adducts with SCIs and RO₂ were detected at high sensitivities:
2,400 ndcps ppbv⁻¹ for SCI·DMPO and 2,000 ndcps ppbv⁻¹ for RO₂·DMPO (Table S1). Sensitivities were experimentally
determined in each ozonolysis experiment and depend on the operational conditions of the PTR3 instrument. Detection limits
for SCI·DMPO and RO₂·DMPO adducts were 3.4×10^7 and 1.6×10^8 molecule cm⁻³, respectively. These limits of detection
are calculated for 30 s integration time as 3 standard deviations of measured background divided by derived sensitivity.

255 In addition, we compare measured concentrations of RO₂·DMPO adducts with the concentrations predicted by the kinetic model (Fig. 7). The observed values are an order of magnitude lower than the modeled ones. Similar to experiments described in Sect. 3.1, several factors can contribute to this discrepancy: (1) gas-wall partitioning of RO₂ species and RO₂·DMPO adducts in the experimental setup and inside the PTR3 instrument; (2) uncertainty in sensitivity at which RO₂·DMPO adducts were detected; (3) potential fragmentation of RO₂·DMPO·NH₄⁺ product ions; and (4) uncertainties in the reaction rate coefficient

260 $k_{\text{RO}_2+\text{DMPO}}$. In our model we assumed that the major fraction of RO₂ species was scavenged by DMPO. This assumption is valid if $k_{\text{RO}_2+\text{DMPO}}$ is larger than $1 \times 10^{-12} \text{ cm}^3 \text{ molecule}^{-1} \text{ s}^{-1}$. Otherwise, other loss channels for peroxy radicals, especially the RO₂+RO₂ reaction, become more important (Fig. S9). Additional experiments under different conditions and intercomparison with established methods (i.e., LIF) are needed to further estimate the measurement capability of the proposed analytical method.

265 Finally, we employed spin trapping for detection of SCIs and organic peroxy radicals formed via ozonolysis of larger cyclic alkenes, such as α -pinene. Decomposition of the α -pinene primary ozonide yields four different C₁₀-SCIs, all of which have the same molecular formula C₁₀H₁₆O₃ (Newland et al., 2018). These SCIs can further isomerize to form primary peroxy radicals C₁₀H₁₅O₄ and OH. Autoxidation of C₁₀H₁₅O₄-RO₂ species can in turn result in formation of several more oxygenated peroxy radicals C₁₀H₁₅O_x, x = 5-9 (Zhao et al., 2018). Signals of SCI·DMPO (C₁₀H₁₆O₃·DMPO) and RO₂·DMPO (C₁₀H₁₅O_x·DMPO,

270 x = 4-9) adducts were observed both in NH₄⁺ and H₃O⁺ CIMS (Figs. 8, S10, S11). OH radicals, formed via decomposition of SCI, can in turn react with α -pinene and lead to formation of OH-derived RO₂ species C₁₀H₁₇O₃ and subsequent autoxidation RO₂ species C₁₀H₁₇O₅ (Berndt et al., 2016). These radicals were detected as the RO₂·DMPO adducts (Figs. S10 and S11). This demonstrates that this analytical method allows for simultaneous detection of a wide range of atmospheric radicals, including the ones with high oxygen content (an O:C ration of up to 0.9) that are formed via autoxidation pathway, and can be

275 used to study kinetics of these species in the laboratory.

4 Conclusions

In summary, we experimentally demonstrated the measurement of speciated, short-lived highly reactive atmospheric compounds, such as Criegee intermediates, organic peroxy radicals and hydroxyl radicals, formed via ozonolysis of alkenes. The analysis was carried out using chemical derivatization techniques, including spin trapping, while the detection of formed

280 radical adducts and closed-shell secondary ozonides was performed by the means of H₃O⁺ and NH₄⁺ CIMS. Detected adducts and secondary ozonides have unique mass defects and can therefore be clearly separated from other observed compounds in the mass spectrum. Implementation of chemical derivatization agents with lower proton affinity allows for the full scavenging and quantification of stabilized Criegee intermediates without depleting CIMS reagent ions. We show that spin traps can be used to effectively scavenge atmospheric radicals and reactive intermediates by demonstrating their high reactivity with

285 radicals in the gas phase using the TEMPO+OH reaction as an example. Using the spin trap DMPO, SCIs and RO₂ species can be simultaneously detected while quantification of observed adducts can be done without their direct calibration. The

detection limits of spin trap and chemical derivatization agent adducts of 1.4×10^7 molecule cm^{-3} for SCIs and 1.6×10^8 molecule cm^{-3} for RO_2 for 30 s integration time were estimated for the instrumentation used here and show promise that these techniques would also work when sampling ambient air. In particular, this method fundamentally enables any CIMS instrument to detect radicals and SCIs. Since spin traps, such as DMPO and TEMPO, are reactive towards a plethora of atmospheric radicals and reactive intermediates, including RO_2 , SCIs, and OH, implementation of such spin traps results in the effective suppression of the radical secondary chemistry and, thus, elimination of potential chemical interferences. The direct method for speciated SCIs and RO_2 measurements provides a means to study the atmospheric chemistry of these compounds. We stress that the quantification of RO_2 species was done under well-defined laboratory conditions using the CID technique such that the estimated sensitivities are likely unique to the electric fields, pressures and flows of the NH_4^+ CIMS instrument. Further validation of the proposed analytical methods in more complex environments closer to the ambient conditions and intercomparison with established methods (i.e., LIF) are needed.

For the future application of the method in field and laboratory experiments, various modifications of the experimental setup can be implemented to improve its measurement capability. We plan to synthesize and test new chemical derivatization agents optimized for the gas-phase measurements with respect to their vapor pressure, selective reactivity and by labelling with atomic isotopes to simplify mass spectrometric detection and improve detection limits. With labeled spin traps, the identification of reactive intermediates may be greatly simplified and detection limits may be further improved, as the spin trap can provide a unique signature in the complex mass-spectrum and move the observed m/z to a region with very low background.

Acknowledgements. This work has received funding from the Harvard Global Institute. Martin Breitenlechner acknowledges support from the Austrian science fund (FWF; grant J-3900). Hendrik Fuchs and Anna Novelli acknowledge support from the European Research Council (ERC) under the European Union's Horizon 2020 research and innovation programme (SARLEP grant agreement No. 681529). Daniel Knopf acknowledges support from the U.S. National Science Foundation (grant no. AGS-1446286). Jesse Kroll acknowledges support from the U.S. National Science Foundation (grant no. AGS-1638672).

Author contributions. FK initially conceived of the work. AZ and MB developed the laboratory setups, performed the experiments, and analyzed the CIMS data. AZ performed the quantum-chemical calculations and wrote the manuscript. AN and HF provided data and analysis for the LP-LIF experiments. DK supported study with PTR-MS measurements. All authors were involved in helpful discussion and contributed to the manuscript.

Data availability. Data used within this work are available upon request. Please email Alexander Zaytsev (zaytsev@g.harvard.edu).

Competing interests. The authors declare that they have no conflict of interest.

320 References

- Bagryanskaya, E.G. and Marque, S.R.: Scavenging of organic C-centered radicals by nitroxides. *Chem. Rev.*, 114(9), 5011-5056, DOI: 10.1021/cr4000946, 2014.
- Berndt, T., Jokinen, T., Sipilä, M., Mauldin III, R.L., Herrmann, H., Stratmann, F., Junninen, H. and Kulmala, M.: H₂SO₄ formation from the gas-phase reaction of stabilized Criegee Intermediates with SO₂: Influence of water vapour content and
325 temperature. *Atmospheric Environment*, 89, 603-612, DOI: 10.1016/j.atmosenv.2014.02.062, 2014.
- Berndt, T., Richters, S., Jokinen, T., Hyttinen, N., Kurtén, T., Otkjær, R.V., Kjaergaard, H.G., Stratmann, F., Herrmann, H., Sipilä, M., Kulmala, M., and Ehn, M.: Hydroxyl radical-induced formation of highly oxidized organic compounds, *Nature Communications*, 7, 13677, DOI: 10.1038/ncomms13677, 2016.
- Berndt, T., Herrmann, H., and Kurten, T.: Direct Probing of Criegee Intermediates from Gas-Phase Ozonolysis Using Chemical
330 ionization Mass Spectrometry, *J. Am. Chem. Soc.*, 139, 13387-13392, DOI: 10.1021/jacs.7b05849, 2017.
- Berndt, T., Mentler, B., Scholz, W., Fischer, L., Herrmann, H., Kulmala, M. and Hansel, A.: Accretion product formation from ozonolysis and OH radical reaction of α -pinene: mechanistic insight and the influence of isoprene and ethylene. *Environmental science & technology*, 52(19), 11069-11077, DOI: 10.1021/acs.est.8b02210, 2018.
- Berndt, T., Hyttinen, N., Herrmann, H., and Hansel, A.: First oxidation products from the reaction of hydroxyl radicals with
335 isoprene for pristine environmental conditions. *Communications Chemistry*, 2(1), 1-10, DOI: 10.1038/s42004-019-0120-9, 2019.
- Breitenlechner, M., Fischer, M., Hainer, M., Heinritzi, M., Curtius, M., and Hansel, A.: PTR3: An instrument for Studying the Lifecycle of Reactive Organic Carbon in the Atmosphere, *Anal. Chem.*, 89, 5824–5831, DOI: 10.1021/acs.analchem.6b05110, 2017.
- 340 Cantrell, C.A., Stedman, D.H., and Wendel, G.J.: Measurement of atmospheric peroxy radicals by chemical amplification, *Anal. Chem.*, 56, 1496–1502. DOI: 10.1021/ac00272a065, 1984.
- Chhantyal-Pun, R., Welz, O., Savee, J.D., Eskola, A.J., Lee, E.P.F., Blacker, L., Hill, H.R., Ashcroft, M., Khan, M.A.H., Lloyd-Jones, G.C., Evans, L., Rotavera, B., Huang, H., Osborn, D.L., Mok, D.K.W., Dyke, J.M., Shallcross, D.E., Percival, C.J., Orr-Ewing, A.J., and Taatjes, C.A.: Direct Measurements of Unimolecular and Bimolecular Reaction Kinetics of the Criegee
345 Intermediate (CH₃)₂COO, *J. Phys. Chem. A*, 121, 4–15, DOI: 10.1021/acs.jpca.6b07810, 2016.
- Drozd, G.T., Kroll, J.H., and Donahue, N.M.: 2,3-Dimethyl-2-butene (TME) Ozonolysis: Pressure Dependence of Stabilized Criegee Intermediates and Evidence of Stabilized Vinyl Hydroperoxides, *J. Phys. Chem. A*, DOI: 10.1021/jp108773d, 2011.
- Drozd, G.T. and Donahue, N.M.: Pressure Dependence of Stabilized Criegee Intermediate Formation from a Sequence of Alkenes, *J. Phys. Chem. A*, DOI: 10.1021/jp2001089, 2011.
- 350 Edwards, G.D., Cantrell, C.A., Stephens, S., Hill, B., Goyea, O., Shetter, R.E., Mauldin III, R.L., Kosciuch, E., Tanner, D.J., and Eisele, F.L.: Chemical Ionization Mass Spectrometer Instrument for the Measurement of Tropospheric HO₂ and RO₂, *Anal. Chem.*, 75, 5317-5327, DOI: 10.1021/ac034402b, 2003.

- Frisch, M. J., Trucks, G. W., Schlegel, H. B., Scuseria, G. E., Robb, M. A., Cheeseman, J. R., Scalmani, G., Barone, V., Mennucci, B., Petersson, G. A., Nakatsuji, H., Caricato, M., Li, X., Hratchian, H. P., Izmaylov, A. F., Bloino, J., Zheng, G., Sonnenberg, J. L., Hada, M., Ehara, M., Toyota, K., Fukuda, R., Hasegawa, J., Ishida, M., Nakajima, T., Honda, Y., Kitao, O., Nakai, H., Vreven, T., Montgomery, J. A., Jr., Peralta, J. E., Ogliaro, F., Bearpark, M., Heyd, J. J., Brothers, E., Kudin, K. N., Staroverov, V. N., Kobayashi, R., Normand, J., Raghavachari, K., Rendell, A., Burant, J. C., Iyengar, S. S., Tomasi, J., Cossi, M., Rega, N., Millam, J. M., Klene, M., Knox, J. E., Cross, J. B., Bakken, V., Adamo, C., Jaramillo, J., Gomperts, R., Stratmann, R. E., Yazyev, O., Austin, A. J., Cammi, R., Pomelli, C., Ochterski, J. W., Martin, R. L., Morokuma, K., Zakrzewski, V. G., Voth, G. A., Salvador, P., Dannenberg, J. J., Dapprich, S., Daniels, A. D., Farkas, Ö., Foresman, J. B., Ortiz, J. V., Cioslowski, J., and Fox, D. J.: Gaussian 09, Revision D.01, Gaussian, Inc.: Wallingford, CT, 2009.
- Fuchs, H., Holland, F., and Hofzumahaus, A.: Measurement of tropospheric RO₂ and HO₂ radicals by a laser-induced fluorescence instrument, *Rev. Sci. Instrum.*, 79, 084104, DOI: 10.1063/1.2968712, 2008.
- Fuchs, H., Novelli, A., Rolletter, M., Hofzumahaus, A., Pfannerstill, E. Y., Kessel, S., Edtbauer, A., Williams, J., Michoud, V., Dusanter, S., Locoge, N., Zannoni, N., Gros, V., Truong, F., Sarda-Esteve, R., Cryer, D. R., Brumby, C. A., Whalley, L. K., Stone, D., Seakins, P. W., Heard, D. E., Schoemaeker, C., Blocquet, M., Coudert, S., Batut, S., Fittschen, C., Thames, A. B., Brune, W. H., Ernest, C., Harder, H., Muller, J. B. A., Elste, T., Kubistin, D., Andres, S., Bohn, B., Hohaus, T., Holland, F., Li, X., Rohrer, F., Kiendler-Scharr, A., Tillmann, R., Wegener, R., Yu, Z., Zou, Q., and Wahner, A.: Comparison of OH reactivity measurements in the atmospheric simulation chamber SAPHIR, *Atmos. Meas. Tech.*, 10, 4023–4053, DOI: 10.5194/amt-10-4023-2017, 2017.
- Giorio, C., Campbell, S.J., Bruschi, M., Tampieri, F., Barbon, A., Toffoletti, A., Tapparo, A., Paijens, C., Wedlake, A.J., Grice, P., Howe, D.J., and Kalberer, M.: Online Quantification of Criegee Intermediates of α -Pinene Ozonolysis by Stabilization with Spin Traps and Proton-Transfer Reaction Mass Spectrometry Detection, *J. Am. Chem. Soc.*, 139, 3999–4008, DOI: 10.1021/jacs.6b10981, 2017.
- Hansel, A., Scholz, W., Mentler, B., Fischer, L. and Berndt, T.: Detection of RO₂ radicals and other products from cyclohexene ozonolysis with NH₄⁺ and acetate chemical ionization mass spectrometry. *Atmospheric Environment*, 186, 248-255, DOI: 10.1016/j.atmosenv.2018.04.023, 2018.
- Hawkins, C.L. and Davies, M.J.: Detection and characterisation of radicals in biological materials using EPR methodology, *Biochimica et Biophysica Acta (BBA)-General Subjects*, 1840(2), 708-721, DOI: 10.1016/j.bbagen.2013.03.034, 2014.
- Horie, O., Schäfer, C. and Moortgat, G.K.: High reactivity of hexafluoro acetone toward criegee intermediates in the gas-phase ozonolysis of simple alkenes. *International journal of chemical kinetics*, 31(4), 261-269, DOI: 10.1002/(SICI)1097-4601(1999)31:4<261::AID-KIN3>3.0.CO;2-Z, 1999.
- Hornbrook, R.S., Crawford, J.H., Edwards, G.D., Goyea, O., Mauldin Iii, R.L., Olson, J.S., Cantrell, C.A: Measurements of tropospheric HO₂ and RO₂ by oxygen dilution modulation and chemical ionization mass spectrometry. *Atmos Meas Tech* 4, 735–756. DOI: 10.5194/amt-4-735-2011, 2011.

- Hunter, E.P. and Lias, S.G.: Evaluated Gas Phase Basicities and Proton Affinities of Molecules: An Update, *J. Phys. Chem. Ref. Data*, 27, 3, 413-656, DOI: 10.1063/1.556018, 1998.
- Isaacman-VanWertz, G., Massoli, P., O'Brien, R.E., Nowak, J.B., Canagaratna, M.R., Jayne, J.T., Worsnop, D.R., Su, L., Knopf, D.A., Misztal, P.K., Arata, C., Goldstein, A.H. and Kroll, J.H.: Using advanced mass spectrometry techniques to fully
390 characterize atmospheric organic carbon: current capabilities and remaining gaps. *Faraday Discussions*, 200, 579-598, DOI: 10.1039/c7fd00021a, 2017.
- Isaacman-VanWertz, G., Massoli, P., O'Brien, R., Lim, C., Franklin, J.P., Moss, J.A., Hunter, J.F., Nowak, J.B., Canagaratna, M.R., Misztal, P.K., Arata, C., Roscioli, J.R., Herndon, S.T., Onasch, T.B., Lambe, A.T., Jayne, J.T., Su, L., Knopf, D.A., Goldstein, A.H., Worsnop, D.R. and Kroll, J.H.: Chemical evolution of atmospheric organic carbon over multiple generations
395 of oxidation. *Nature Chem.*, 10, 462-468, DOI: 10.1038/s41557-018-0002-2, 2018.
- Jenkin, M.E., Saunders, S.M., Pilling, M.J.: The tropospheric degradation of volatile organic compounds: a protocol for mechanism development, *Atmos. Environ.*, 31, 81-104, DOI: 10.1016/S1352-2310(96)00105-7, 1997.
- Johnson, D. and Marston, G.: The gas-phase ozonolysis of unsaturated volatile organic compounds in the troposphere. *Chemical Society Reviews*, 37(4), 699-716, DOI: 10.1039/b704260b, 2008.
- 400 Khan, M.A.H., Percival, C.J., Caravan, R.L., Taatjes, C.A. and Shallcross, D.E.: Criegee intermediates and their impacts on the troposphere, *Environ. Sci.: Processes Impacts*, 20, 437, DOI: 10.1039/C7EM00585G, 2018.
- Lewis, T.R., Blitz, M.A., Heard, D.E. and Seakins, P.W.: Direct evidence for a substantive reaction between the Criegee intermediate, CH₂OO, and the water vapour dimer. *Physical Chemistry Chemical Physics*, 17(7), 4859-4863, DOI: 10.1039/C4CP04750H, 2015.
- 405 Long, B., Bao, J.L., and Truhlar, D.G. Unimolecular reaction of acetone oxide and its reaction with water in the atmosphere, *PNAS*, 115, 6135-6140, DOI: 10.1073/pnas.1804453115, 2018.
- Lou, S., Holland, F., Rohrer, F., Lu, K., Bohn, B., Brauers, T., Chang, C. C., Fuchs, H., Häsel, R., Kita, K., Kondo, Y., Li, X., Shao, M., Zeng, L., Wahner, A., Zhang, Y., Wang, W., and Hofzumahaus, A.: Atmospheric OH reactivities in the Pearl River Delta – China in summer 2006: measurement and model results, *Atmos. Chem. Phys.*, 10, 11243–11260,
410 <https://doi.org/10.5194/acp-10-11243-2010>, 2010.
- Mihelcic, D., Müsgen, P., and Ehhalt, D.H.: An improved method of measuring tropospheric NO₂ and RO₂ by matrix isolation and electron spin resonance, *J. Atmos. Chem.*, 3, 341-361, DOI: 10.1007/BF00122523, 1985.
- Murray, R.W., Story, P.R., and Loan, L.D.: Ozonides from Aldehydic Zwitterions and Acetone, *J. Am. Chem. Soc.* 87, 13, 3025-3026, DOI: 10.1021/ja01091a054, 1965.
- 415 Neeb, P., Sauer, F., Horie, O., and Moortgat, G. K.: Formation of hydroxymethyl hydroperoxide and formic acid in alkene ozonolysis in the presence of water vapour, *Atmos. Environ.*, 31, 1417– 1423, DOI: 10.1016/S1352-2310(96)00322-6, 1997.
- Newland, M.J., Rickard, A.R., Alam, M.S., Vereecken, L., Munoz, A., Rodenas, M. and Bloss, W.J.: Kinetics of stabilised Criegee intermediates derived from alkene ozonolysis: reactions with SO₂, H₂O and decomposition under boundary layer conditions. *Phys. Chem. Chem. Phys.*, 17, 4076-4088, DOI: 10.1039/C4CP04186K, 2015.

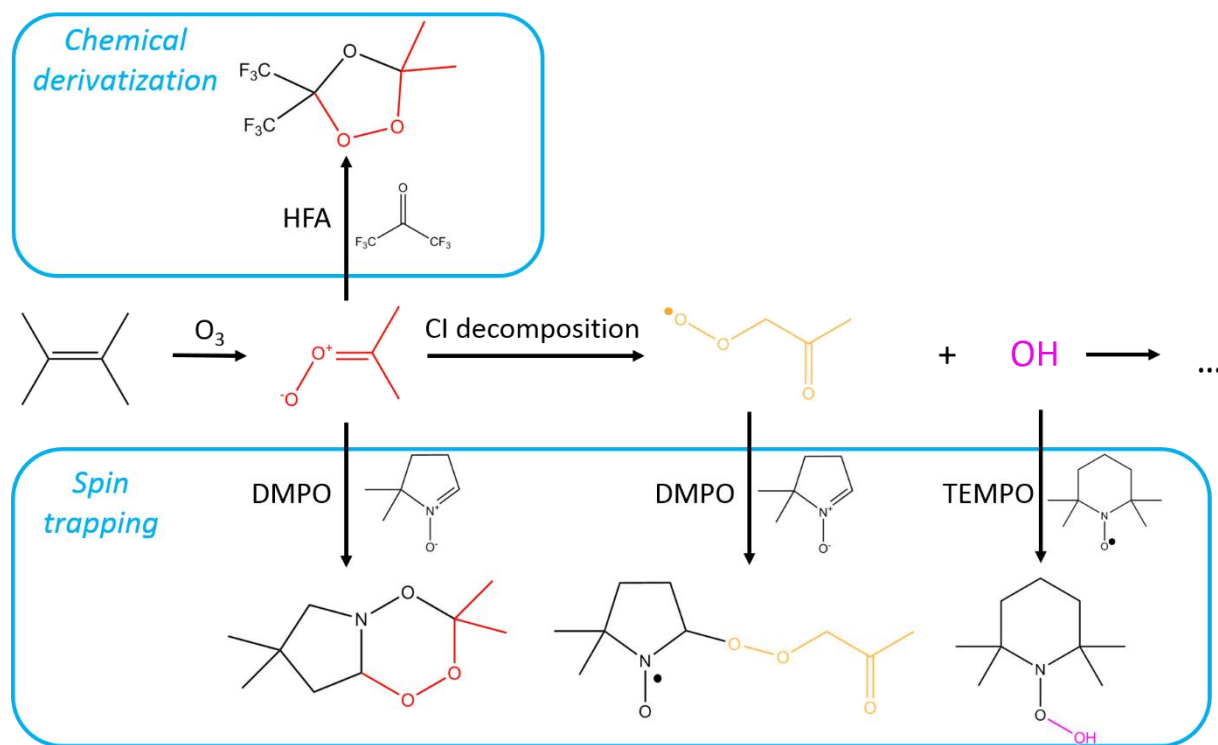
- 420 Newland, M. J., Rickard, A. R., Sherwen, T., Evans, M. J., Vereecken, L., Muñoz, A., Ródenas, M., and Bloss, W. J.: The atmospheric impacts of monoterpene ozonolysis on global stabilised Criegee intermediate budgets and SO₂ oxidation: experiment, theory and modelling, *Atmos. Chem. Phys.*, 18, 6095–6120, DOI: 10.5194/acp-18-6095-2018, 2018.
- Nosaka, Y. and Nosaka, A.Y.: Generation and detection of reactive oxygen species in photocatalysis, *Chem. Rev.*, 117(17), 11302-11336, DOI: 10.1021/acs.chemrev.7b00161, 2017.
- 425 Novelli, A., Hens, K., Tatum Ernest, C., Martinez, M., Nölscher, A. C., Sinha, V., Paasonen, P., Petäjä, T., Sipilä, M., Elste, T., Plass-Dülmer, C., Phillips, G. J., Kubistin, D., Williams, J., Vereecken, L., Lelieveld, J., and Harder, H.: Estimating the atmospheric concentration of Criegee intermediates and their possible interference in a FAGE-LIF instrument, *Atmos. Chem. Phys.*, 17, 7807–7826, DOI: 10.5194/acp-17-7807-2017, 2017.
- Nozière, B. and Vereecken, L.: Direct Observation of Aliphatic Peroxy Radical Autoxidation and Water Effects: An
430 Experimental and Theoretical Study. *Angew. Chem.*, 58(39), 13976-13982, DOI: 10.1002/anie.201907981, 2019.
- Orlando, J.J., and Tyndall, G.S.: Laboratory studies of organic peroxy radical chemistry: an overview with emphasis on recent issues of atmospheric significance, *Chem. Soc. Rev.*, 41, 6294–6317, DOI: 10.1039/c2cs35166h, 2012.
- Pattison, D.I., Lam, M., Shinde, S.S., Anderson, R.F. and Davies, M.J.: The nitroxide TEMPO is an efficient scavenger of protein radicals: Cellular and kinetic studies. *Free Radical Biology and Medicine*, 53, 1664–1674, DOI:
435 10.1016/j.freeradbiomed.2012.08.578, 2012.
- Pagonis, D., Krechmer, J. E., de Gouw, J., Jimenez, J. L., and Ziemann, P. J.: Effects of gas–wall partitioning in Teflon tubing and instrumentation on time-resolved measurements of gas-phase organic compounds, *Atmos. Meas. Tech.*, 10, 4687–4696, DOI: 10.5194/amt-10-4687-2017, 2017.
- Reiner, T., Hanke, M. and Arnold, F.: Atmospheric peroxy radical measurements by ion molecule reaction-mass spectrometry:
440 A novel analytical method using amplifying chemical conversion to sulfuric acid. *Journal of Geophysical Research: Atmospheres*, 102(D1), 1311-1326, DOI: 10.1029/96JD02963, 1997.
- Roberts, J.G., Voinov, M.A., Schmidt, A.C., Smirnova, T.I. and Sombers, L.A.: The hydroxyl radical is a critical intermediate in the voltammetric detection of hydrogen peroxide. *J. Am. Chem. Soc.*, 138(8), 2516-2519, DOI: 10.1021/jacs.5b13376, 2016.
- Samuni, A., Goldstein, S., Russo, A., Mitchell, J.B., Krishna, M.C. and Neta, P.: Kinetics and mechanism of hydroxyl radical
445 and OH-adduct radical reactions with nitroxides and with their hydroxylamines. *J. Am. Chem. Soc.*, 124(29), 8719-8724, DOI: 10.1021/ja017587h, 2002.
- Saunders, S. M., Jenkin, M. E., Derwent, R. G., and Pilling, M. J.: Protocol for the development of the Master Chemical Mechanism, MCM v3 (Part A): tropospheric degradation of non-aromatic volatile organic compounds, *Atmos. Chem. Phys.*, 3, 161–180, DOI: 10.5194/acp-3-161-2003, 2003.
- 450 Sipilä, M., Jokinen, T., Berndt, T., Richters, S., Makkonen, R., Donahue, N. M., Mauldin III, R. L., Kurtén, T., Paasonen, P., Sarnela, N., Ehn, M., Junninen, H., Rissanen, M. P., Thornton, J., Stratmann, F., Herrmann, H., Worsnop, D. R., Kulmala, M., Kerminen, V.-M., and Petäjä, T.: Reactivity of stabilized Criegee intermediates (sCIs) from isoprene and monoterpene ozonolysis toward SO₂ and organic acids, *Atmos. Chem. Phys.*, 14, 12143–12153, DOI: 10.5194/acp-14-12143-2014, 2014.

- Stephens, P. J., Devlin, F. J., Chabalowski, C. F. N., and Frisch, M. J.: Ab initio calculation of vibrational absorption and circular dichroism spectra using density functional force fields. *The Journal of physical chemistry*, 98, 11623-11627, DOI: 10.1021/j100096a001, 1994.
- Taatjes, C.A., Meloni, G., Selby, T.M., Trevitt, A.J., Osborn, D.L., Percival, C.J. and Shallcross, D.E.: Direct observation of the gas-phase Criegee intermediate (CH_2OO). *J. Am. Chem. Soc.*, 130(36), 11883-11885, DOI: 10.1021/ja804165q, 2008.
- Taatjes, C.A., Welz, O., Eskola, A.J., Savee, J.D., Osborn, D.L., Lee, E.P.F., Dyke, J.M., Mok, D.W.K., Shallcross D.E., and Percival, C.J.: Direct measurement of Criegee intermediate (CH_2OO) reactions with acetone, acetaldehyde, and hexafluoroacetone, *Phys. Chem. Chem. Phys.*, 14, 10391–10400, DOI: 10.1039/C2CP40294G, 2012.
- Van Der Zee, J., Barr, D.P. and Mason, R.P.: ESR spin trapping investigation of radical formation from the reaction between hematin and tert-butyl hydroperoxide. *Free Radical Biology and Medicine*, 20(2), 199-206, DOI: 10.1016/0891-5849(95)02031-4, 1996.
- Vereecken, L., Novelli, A. and Taraborrelli, D.: Unimolecular decay strongly limits the atmospheric impact of Criegee intermediates. *Phys. Chem. Chem. Phys.*, 19(47), 31599-31612, DOI: 10.1039/C7CP05541B, 2017.
- Watanabe, T., Yoshida, M., Fujiwara, S., Abe, K., Onoe, A., Hirota, M. and Igarashi, S.: Spin trapping of hydroxyl radical in the troposphere for determination by electron spin resonance and gas chromatography/mass spectrometry. *Anal. Chem.*, 54(14), 2470-2474, DOI: 10.1021/ac00251a015, 1982.
- Welz, O., Savee, J.D., Osborn, D.L., Vasu, S.S., Percival, C.J., Shallcross, D.E., and Taatjes, C.A.: Direct kinetic measurements of Criegee intermediate (CH_2OO) formed by reaction of CH_2I with O_2 , *Science*, 335, 204-207, DOI: 10.1126/science.1213229, 2012.
- Wolfe, G. M., Marvin, M. R., Roberts, S. J., Travis, K. R., and Liao, J.: The Framework for 0-D Atmospheric Modeling (F0AM) v3.1, *Geosci. Model Dev.*, 9, 3309–3319, DOI: 10.5194/gmd-9-3309-2016, 2016.
- Womack, C.C., Martin-Drumel, M.A., Brown, G.G., Field, R.W. and McCarthy, M.C.: Observation of the simplest Criegee intermediate CH_2OO in the gas-phase ozonolysis of ethylene. *Sci. Adv.*, 1(2), DOI: 10.1126/sciadv.1400105, 2015.
- Wood, E.C. and Charest, J.R.: Chemical amplification - cavity attenuated phase shift spectroscopy measurements of atmospheric peroxy radicals. *Anal. Chem.* 86, 10266–10273. DOI: 10.1021/ac502451m, 2014.
- Wright, P.J. and English, A.M.: Scavenging with TEMPO• to identify peptide-and protein-based radicals by mass spectrometry: Advantages of spin scavenging over spin trapping. *Journal of the American Chemical Society*, 125(28), 8655-8665, DOI: 10.1021/ja0291888, 2003.
- Yuan, B., Koss, A.R., Warneke, C., Coggon, M., Sekimoto, K., and de Gouw, J.A.: Proton-Transfer-Reaction Mass Spectrometry: Applications in Atmospheric Sciences, *Chem. Rev.*, 117, 13187–13229, DOI: 10.1021/acs.chemrev.7b00325, 2017.
- Zaytsev, A., Breitenlechner, M., Koss, A. R., Lim, C. Y., Rowe, J. C., Kroll, J. H., and Keutsch, F. N.: Using collision-induced dissociation to constrain sensitivity of ammonia chemical ionization mass spectrometry (NH_4^+ CIMS) to oxygenated volatile organic compounds, *Atmos. Meas. Tech.*, 12, 1861–1870, DOI: 10.5194/amt-12-1861-2019, 2019.

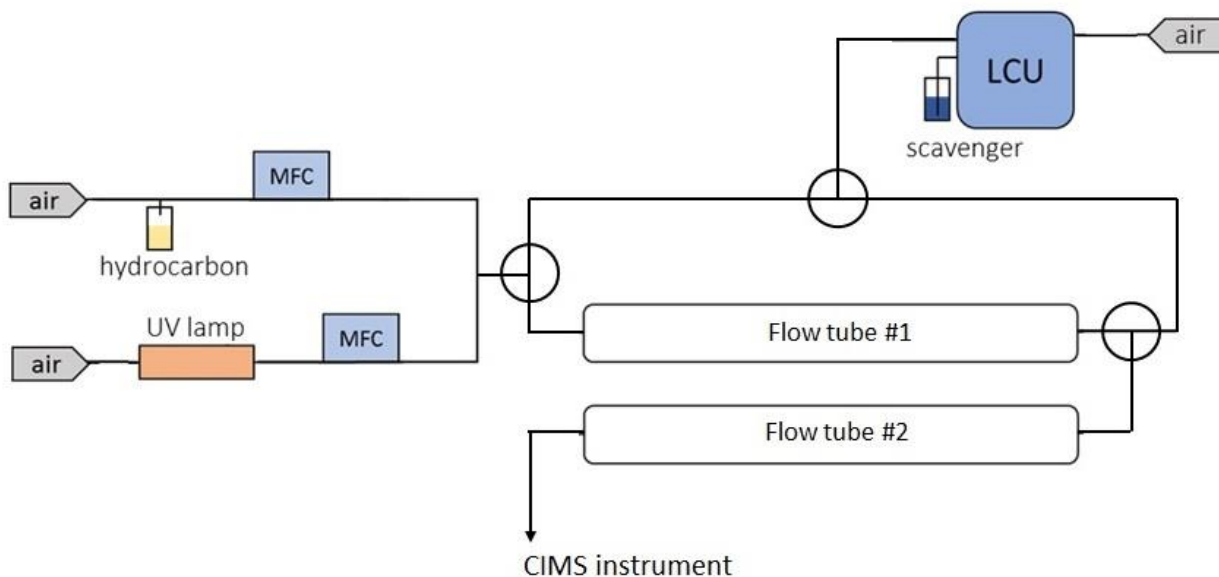
Zhao, Y., Thornton, J.A., and Pye, H.O.: Quantitative constraints on autoxidation and dimer formation from direct probing of monoterpene-derived peroxy radical chemistry. *Proceedings of the National Academy of Sciences*, 115, 12142-12147, DOI: 10.1073/pnas.1812147115, 2018.

Table 1: Proton affinities (PAs) of HFA, water and secondary ozonides produced in reactions of SCIs with HFA. Species with PAs higher than that of water can be detected in H₃O⁺ CIMS.

Species	PA, kcal/mol	Reference
CH ₂ OO·HFA	662.9	This work
HFA	670.4	Hunter and Lias (1998)
H ₂ O	691	Hunter and Lias (1998)
CH ₃ CH ₂ CHOO·HFA	720.7	This work
CH ₃ CH ₂ CH ₂ CHOO·HFA	730.8	This work
(CH ₃) ₂ COO·HFA	747.2	This work
(CH ₂ =C(CH ₃))CHOO·HFA	779.6	This work

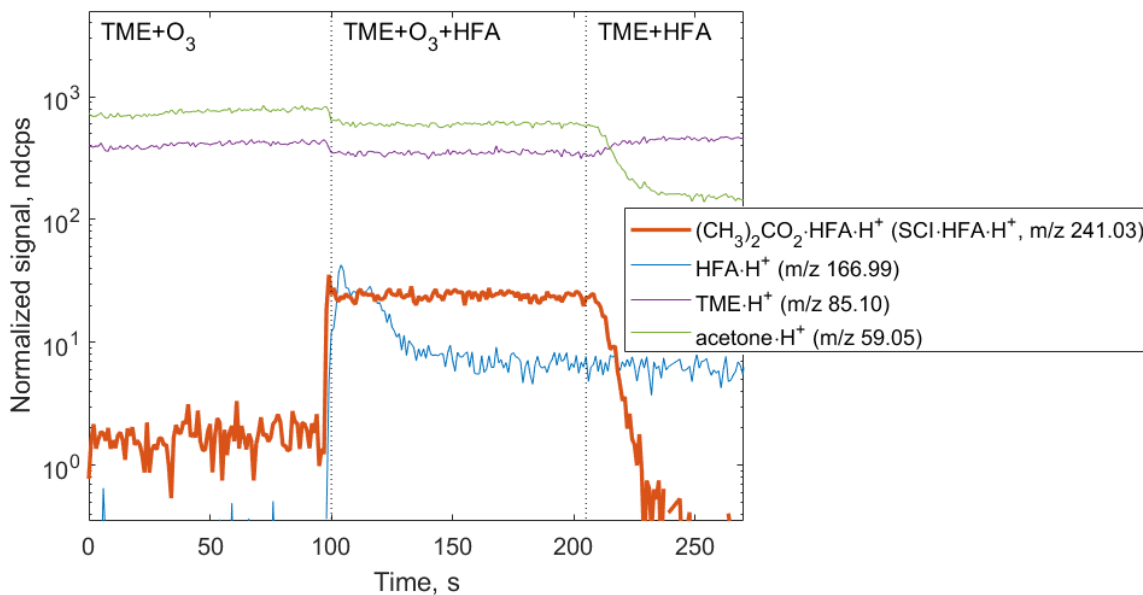


495 **Figure 1: Mechanism of tetramethylethylene (TME) ozonolysis. Stabilized Crigee intermediate (shown in red) can be scavenged by the chemical derivatization agent HFA or the spin trap DMPO, or decompose to peroxy radical (shown in yellow) and OH. RO₂ and OH species can in turn react with spin traps. Reactions involving SCI are from MCM v3.3.1 (Jenkin et al., 1997) and Giorio et al. (2017).**



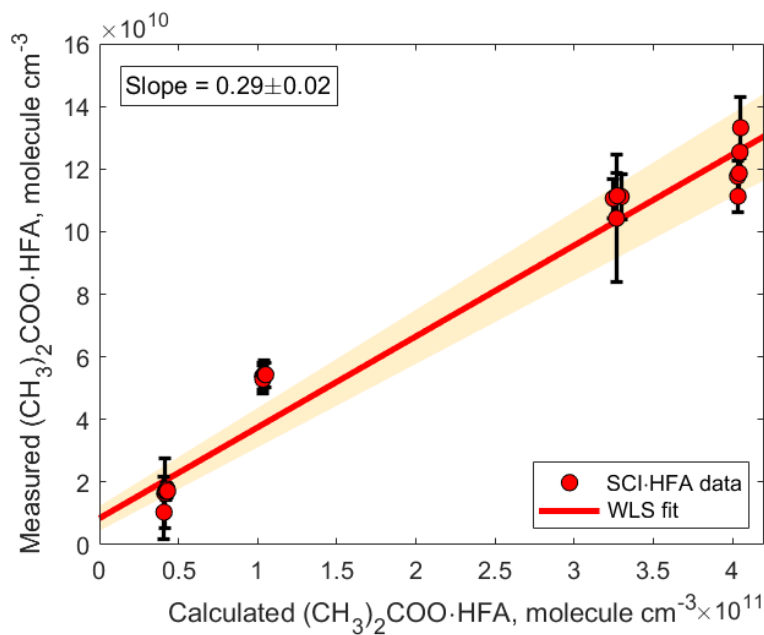
500

Figure 2: Schematic of experimental setup used to detect SCIs and RO₂ with the spin trap DMPO. DMPO was introduced in the experimental setup using a liquid calibration unit (LCU, IONICON Analytik).

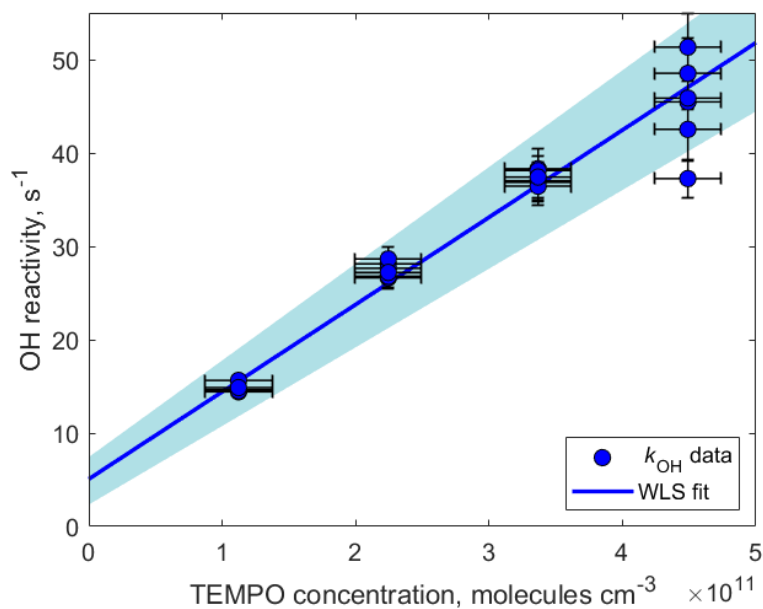


505

Figure 3: Ion tracers observed in a TME ozonolysis experiment as a function of different reactant conditions. Reactant concentrations are [TME] = 1.85×10^{12} ; [O₃] = 1.67×10^{13} ; [HFA] = 6.09×10^{15} molecule cm⁻³. (CH₃)₂COO·HFA·H⁺ ion (red tracer, *m/z* 241.03) is observed when TME, HFA, and O₃ are present in the system.



510 **Figure 4: Correlation plot comparing measured and calculated concentrations of $(\text{CH}_3)_2\text{COO}\cdot\text{HFA}$. The adducts were detected using H_3O^+ CIMS as $(\text{CH}_3)_2\text{COO}\cdot\text{HFA}\cdot\text{H}^+$ (m/z 241.03). The slope is calculated using weighted least squares (WLS). A 95% confidence interval is estimated via a Monte Carlo simulation ($N=5000$) and shown using red shading.**



515 **Figure 5: OH reactivity measured as a function of TEMPO concentration. The slope determining the reaction rate coefficient $k_{\text{TEMPO}+\text{OH}} = (9.3 \pm 0.9) \times 10^{-11} \text{ cm}^3 \text{ molecule}^{-1} \text{ s}^{-1}$ is calculated using weighted least squares (WLS). A 95% confidence interval is estimated via a Monte Carlo simulation ($N=5000$) and shown using blue shading. The intercept $(5.1 \pm 2.4) \text{ s}^{-1}$ can be explained by other OH reactants such as O_3 , NO , NO_2 , and CO .**

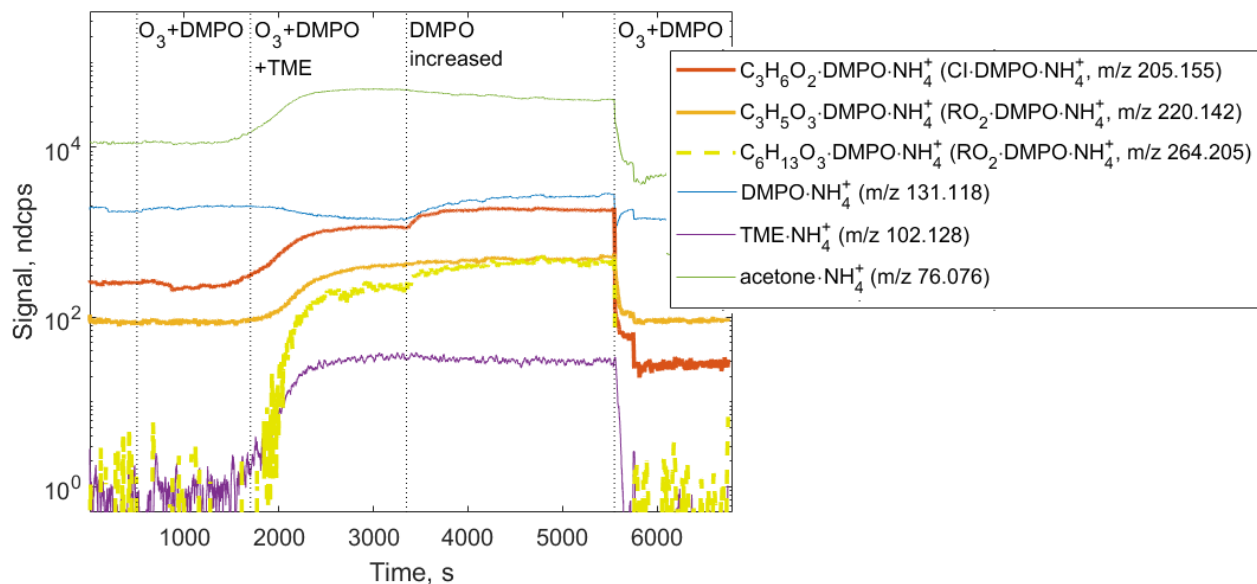
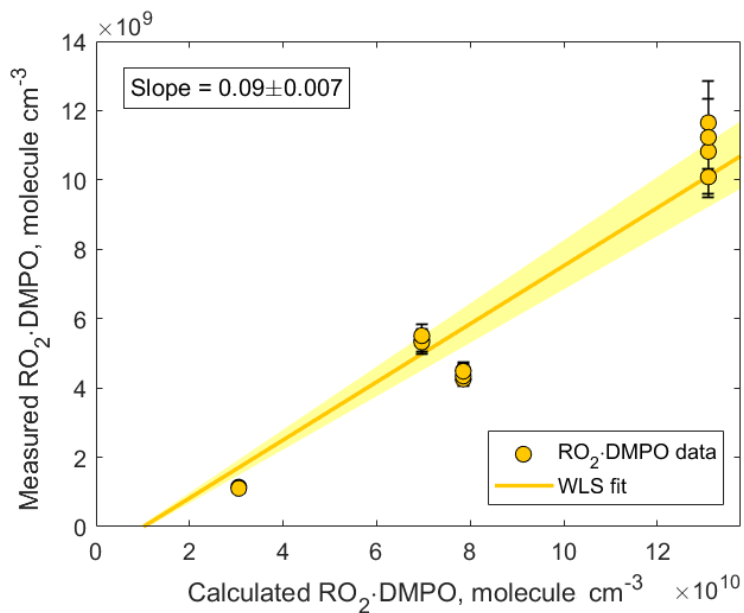
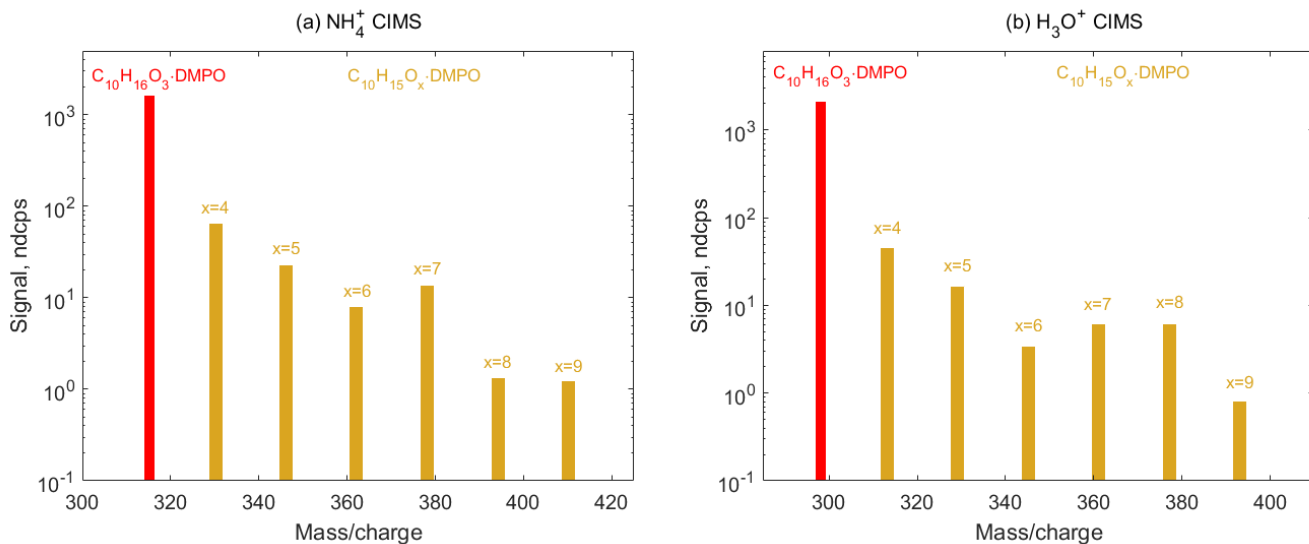


Figure 6: Ion tracers observed by NH_4^+ CIMS in a TME ozonolysis experiment as a function of different reactant conditions. Reactant concentrations are $[\text{TME}] = 3.69 \times 10^{11}$; $[\text{O}_3] = 7.87 \times 10^{12}$; $[\text{DMPO}] = 2.01 \times 10^{12}$ molecule cm^{-3} .



520 **Figure 7:** Correlation plot comparing measured and calculated concentrations of $\text{CH}_3\text{C}(=\text{O})\text{CH}_2\text{OO}\cdot\text{DMPO}$. The adducts were detected using NH_4^+ CIMS as $\text{CH}_3\text{C}(=\text{O})\text{CH}_2\text{OO}\cdot\text{DMPO}\cdot\text{NH}_4^+$ (m/z 220.142). The slope is calculated using weighted least squares (WLS). A 95% confidence interval is estimated via a Monte Carlo simulation ($N=5000$) and shown using yellow shading.



525 **Figure 8:** Mass spectra of SCI·DMPO (red) and RO₂·DMPO (yellow) adducts in α -pinene ozonolysis experiments observed using (a) NH_4^+ CIMS and (b) H_3O^+ CIMS. Primary RO₂ species ($\text{C}_{10}\text{H}_{15}\text{O}_4$) are formed via CI isomerization and can in turn undergo various autoxidation reactions resulting in formation of several organic peroxy radicals ($\text{C}_{10}\text{H}_{15}\text{O}_x$, $x=5-9$), which were detected bas adducts with the spin trap DMPO by the means of NH_4^+ and H_3O^+ CIMS.